Nonlinear Oscillation for a Millimeter-sized Electrostatic Energy Harvester

Kazuyohi Ono*, Norio Sato**, Tomomi Sakata**, Yoshito Jin*·**, Yasuhiro Sato**, and Hiroshi Koizumi*
*NTT Device Technology Laboratories, **NTT Device Innovation Center,
Nippon Telegraph and Telephone Corporation
3-1, Morinosato Wakamiya, Atsugi-shi, Kanagawa Pref. 243-0198, Japan
E-mail:ono.kazuyoshi@lab.ntt.co.jp

***Abstract*— This paper describes a demonstration of power enhancement by nonlinear oscillation in a millimeter-sized electrostatic vibrational energy harvester for the future Internet of Things. To attain nonlinearity in the microelectromechanical-system (MEMS) device, a gold spring, which has a lower value of Young's modulus than conventional materials, is adopted as a component of the MEMS structure. The nonlinear oscillation for the millimeter-sized ethylene tetrafluoroethylene (ETFE) electret energy harvester was confirmed experimentally by applying external vibration. The normalized harvester's effectiveness for the nonlinear oscillation is 9.6 times higher than that for the linear one.**

Keywords— energy harvest; electret; nonlinear; vibration; MEMS; ETFE; Internet of Things

I. INTRODUCTION

The Internet of Things (IoT) can be defined as a new dynamic network of networks, where every day daily objects can communicate with each other [1]. Furthermore, in the IoT, objects can also sense the environment and potentially act on it. Therefore, technologies for wireless sensor networks (WSNs) are intensively being developed. Sensor nodes normally operate with a battery, and if the battery dies, they are unavailable until the battery is replaced [2]. In order to solve the problem, energy harvesting (EH) is attracting much attention [3]. We have proposed various energy harvesting technologies, such as a MEMS vibrational energy harvesting device [4-7], nanowatt-level power management circuit [8,9], and CMOS- MEMS integration process [10] for a small sensor node. Realizing autonomous sensor nodes requires, not only low-power operation of the circuit, but also a power enhancement for the energy harvester. As one solution, some groups have proposed a nonlinear effect for vibrational energy harvesting [11-16]. On the basis of this principle, a large-scale prototype with a size on a centimeter order has been fabricated. To integrate the harvester in a small sensor node, the harvester should be scaled down further. In this paper, we demonstrate power enhancement by nonlinear oscillation in a millimeter-sized electrostatic vibrational energy harvester using our CMOS-MEMS integration technologies for the future IoT.

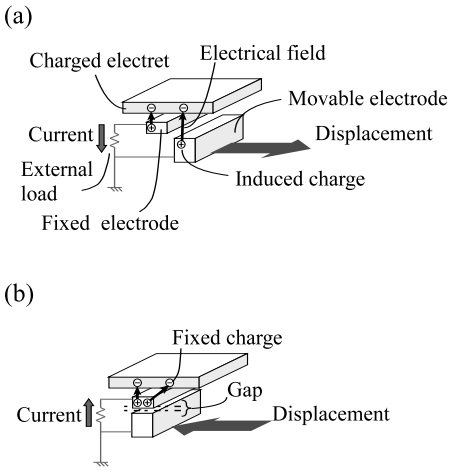

Fig. 1. Fundamental mechanism of current generation based on electrostatic induction:(a) act of displacement from initial state and (b) act of displacement to initial state in the unit cell.

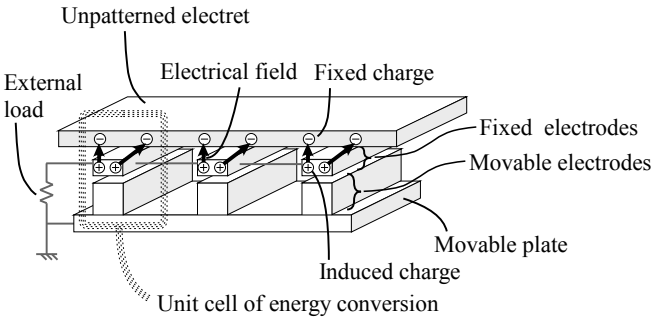

Fig. 2. Concept of our slit-and-slider structure.

II. PRINCIPLE

A. Electrostatic energy harvesting

Three types of vibrational energy conversions have been studied namely piezoelectric, electromagnetic, and electrostatic induction. Electrostatic induction is a promising mechanism

because it is compatible with the CMOS-LSI process [17]. An electrostatic-type energy harvester employs the phenomenon of electrostatic induction in a dielectric. And a good dielectric material to use is an electret, which can be charged to a high voltage and can hold that voltage semi-permanently. Figure 1 shows the principle of electrostatic energy harvesting with an electret. The electret induces electrical charges on the fixed electrode and the movable electrode [Fig.1(a)]. When the movable electrode plate is displaced in the direction of the arrow, some of the positive charges move between the fixed and movable electrodes, and then current is generated through the external load [Fig.1(b)].

Figure 2 shows the fundamental concept of the slit-and-slider structure we have proposed [4-7]. Fixed negative charges in an electret film induce counter positive charges in the movable and fixed electrodes. In the initial state, the fixed electrodes and movable electrodes are aligned vertically. A number of unit cells for energy conversion are aligned across the movable plate in a horizontal direction (See Fig.1) for energy conversion in one movement period.

B. Nonlinear spring effect

The general equation for a single-degree-of-freedom oscillator excited by base acceleration may be formulated from the physical coordinates where the relative displacement *X(t)* of an inertial mass *m* is determined by

$$m\ddot{X} + c\dot{X} + \frac{dU(X)}{dX} = -m\ddot{Z} \tag{1}$$

where c is the viscous damping constant, $\ddot{Z}$ is the input base acceleration, and the overdot denotes differentiation with time [14]. The restoring force potential of the oscillator is expressed as

$$U(X) = \frac{1}{2}k_1(1-r)X^2 + \frac{1}{4}k_3X^4 \tag{2}$$

where k_1 is the linear spring constant, k_3 is the nonlinear spring constant, and r is a tuning parameter. A nondimensional time $\tau = \omega t$, is applied to (2), where $\omega = \sqrt{k_1/m}$ is the linear natural frequency of the oscillator. Defining $\zeta = c/2m\omega$, as operator $\dot{x}$ to x' as differentiation with respect to τ, the nondimensional general equation is given as

$$x'' + 2\zeta x' + (1-r)x + \delta x^3 = -z''. \tag{3}$$

Equation (3) is the Duffing equation, which has a rich history [14]. When the system is driven strongly, the Duffing nonlinearity causes the resonance response curve to become asymmetric. When the resonance is pulled far enough to one side, hysteretic behavior is observed as two stable states appear in the system [15]. The dominant source of nonlinearity in a vibrational device is the additional tension in the spring that appears when vibrations are sufficiently large.

III. STRUCUTRE

Figure 3 shows the basic components of the slit-and-slider structure of a vibrational energy harvester that we have already proposed [4-7]. This structure consists of a slit chip (upper chip) and a slider chip (lower chip). The slit chip contains a charged electret film, a fixed electrode, and a supporting substrate. The slider chip contains a lower wall and a movable part, which consists of a movable electrode suspended by springs through anchors, on a substrate. The features of this structure are as follows: it ensures an arbitrary gap between the fixed and movable electrodes by controlling the height of two walls that separate the slit and slider chips; it integrates composing elements used for vibrational energy harvesting in slit and slider chips; and it uses a wall to protect the movable part on the slider chip from various kinds of external contaminations, such as dust and moisture. Each chip is connected by means of two walls using a conventional flip-chip assembly, which has often been employed in MEMS device fabrication. By designing the parameters of the springs, such as shape and material, we can control the emergence of nonlinearity.

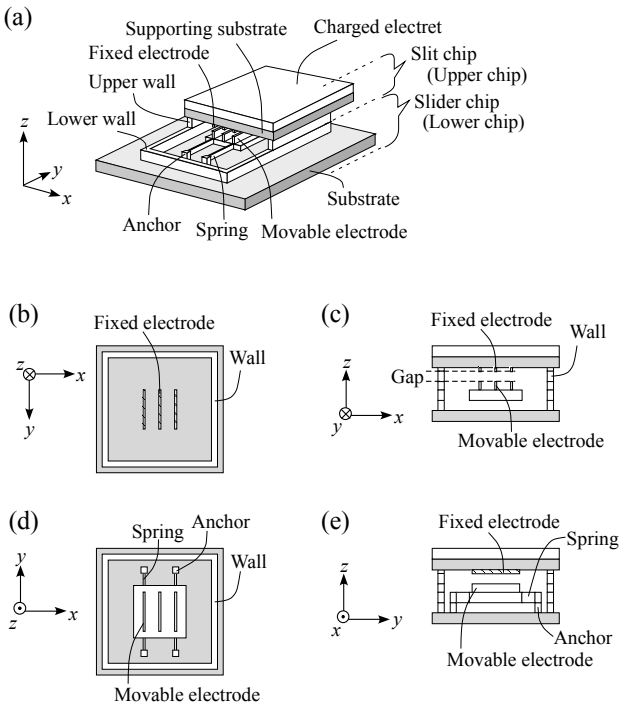

Fig. 3. Basic components of a slit-and-slider structure: (a) bird's eye view, (b) cross-section view of y-z plane, (c) top view of slit chip, (d) cross-section view of x-z plane, and (e) top view of slider chip.

IV. EXPERIMENTAL PROCEDURE

A. Device fabrication

Figure 4 outlines the fabrication process. The structure consists of an electret, an upper chip, and a lower chip. First, the movable structure, springs, stopper, and walls are fabricated on the lower chip by a stacking technique using 10-μm-thick-level gold electroplating on the Si wafer on which

interconnection layers has been formed [Fig. 4(a)]. Next, the sacrificial layers are removed by ashing [Fig. 4(b)]. The upper chip is fabricated by gold electroplating [Fig. 4(c)] and mounted on the lower chip by flip-chip bonding [Fig. 4(d)]. After that, the charged electret film is mounted on the upper chip.

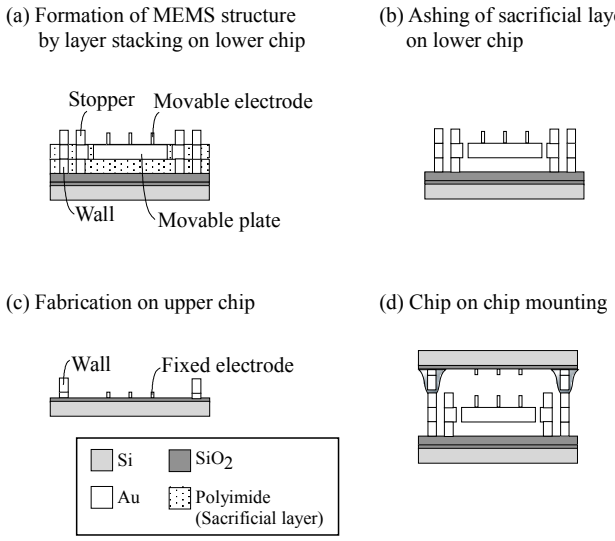

Fig. 4. Fabrication process for slit-and-slider structure.

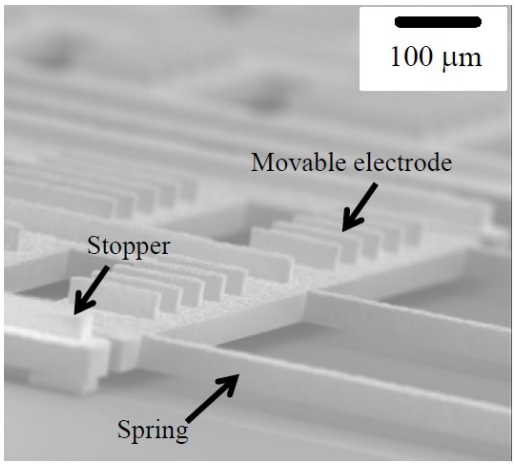

Fig. 5. Fabricated movable structure on lower chip.

Figure 5 shows a scanning electron microscope (SEM) image of the fabricated movable structure on the lower chip. The image clearly shows that the movable plate and stopper are flat, which means that the movable structure is formed without warpage. In addition, the springs are formed without unnecessary bending.

B. Current generation

To confirm the nonlinearity for energy harvesting, current generation was measured by the induction of external vibration as shown in Fig. 6. An electret film, ethylene-tetrafluorinated ethylene copolymer (ETFE), was sandwiched between the top of the MEMS vibrational device and a metal plate. We used a 100-μm-thick ETFE film whose permittivity and dielectric tangent are 2.6 and 0.0008 at 1 kHz, respectively. The film was subjected to a DC corona discharge at a bias voltage of -10 kV and room temperature. The average potentials on the surface and rear side of the charged film around the area above the movable plate were about -900 and +780 V, respectively. From these potentials, the charge densities were calculated with $\sigma = \varepsilon_0 \varepsilon V/d$ as -20.7 and 17.9 nC/cm^2, respectively, where we used the values as the dielectric permittivity of vacuum $\varepsilon_0 = 8.85\times10^{-12}$ F/m, the relative permittivity of the ETFE ε = 2.6, the potential V, and thickness of the electret film d = 100 μm. The fixed electrodes and metal plate were directly grounded. The movable electrodes were also grounded through the lock-in amplifier, which has an impedance of 1 kΩ. The lock-in amplifier detected the current signal synchronized with an input vibrational reference signal. The external vibration frequency was swept from 1200 to 1280 Hz while the acceleration was changed from 1 to 5 m/s^2, as found in practical environments [17].

Figure 7(a) shows the frequency response with the acceleration for external mechanical vibration as the parameter. The AC current shows a peak at each parameter. Figure 7(b) shows the phase difference between the output of the device and the input signal of the applied vibration. Each phase corresponding to the acceleration changes reversely from 1218 to 1238 Hz, which confirms that each peak corresponding to the current in Fig. 7(a) originated from resonance. For acceleration = 1 m/s^2, the shape of the frequency response is symmetric on both sides of the peak, while for more than 2 m/s^2, the peak is not symmetric. Also, the bandwidths for linear and nonlinear oscillation are 7 and 15 Hz, respectively. Owing to this nonlinearity, the band of the spectrum is broadened. From this result, nonlinear operation for electrostatic energy harvesting is demonstrated.

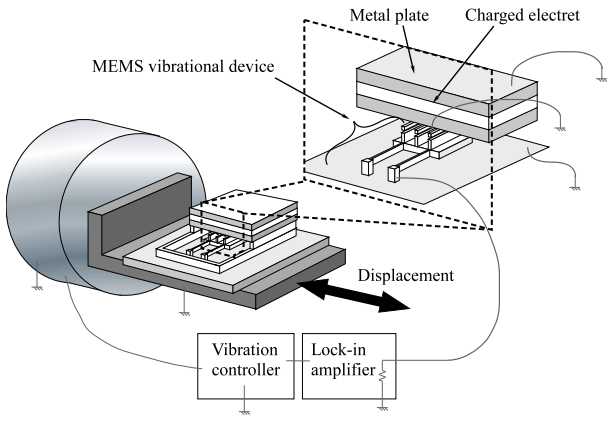

Fig. 6. Experimental setup for current generation.

V. DISCUSSION

To compare the generated output of the nonlinear oscillation with that of the linear one, the harvester's effectiveness is introduced from ref [7] as

$$E_H = \frac{Useful\ Power\ Output}{Maximum\ Possible\ Output} = \frac{Useful\ Power\ Output}{\frac{1}{2}aZ_1\omega m} \quad (4)$$

where a, Z_l, ω, and m are acceleration, maximum displacement, angular frequency of source motion, and proof mass respectively. In this formula, the Useful Power Output, which is extracted from the actual experiments, is normalized by the applied external power as the Maximum Possible Output. Therefore, we can evaluate the effectiveness of energy harvesting with this E_H [7]. The useful power output of a harvester is obtained as

$$P_{\exp} = R_L \bar{I}^2 \quad . \quad (5)$$

Here, the maximum possible output means kinetic energy for the vibrational devices. With this expression, we can compare the nonlinear one with the linear one as a normalized value for external input such as the acceleration and frequency.

Table I shows the calculated useful power output and its related value from the experiment as shown in Fig. 7. Also, the effectiveness was calculated from (4) as shown in Table II. The values of effectiveness for the nonlinear and linear are 1.08×10^{-7} and 1.18×10^{-8}, respectively. The ratio is 9.6, which means that the nonlinear operation is 9.6 times more effective than the linear one. It was demonstrated experimentally that nonlinear operation broadens the band of the spectrum and boosts the current, indicating that this technique is effective for improving the power enhancement for small energy harvester. These results indicate significant progress as regards miniaturized MEMS energy harvesters for wireless sensor nodes in the future Internet of Things.

TABLE I. THE CALCULATED USEFUL POWER OUTPUT AND ITS RELATED VALUE FROM EXPERIMENT

Condition	***I [A]***	***R_L [Ω]***	***P_{exp} [W]***
Nonlinear	4.93×10^{-9}	1×10^{3}	2.40×10^{-14}
Linear	6.98×10^{-10}	1×10^{3}	4.87×10^{-16}

TABLE II. THE CALCULATED EFFECTIVENESS FROM EQUATION (4)

Condition	***f [Hz]***	***a [m/s^2]***	***P_{max} [W]***	***E_H***
Nonlinear	1238	5	2.40×10^{-14}	1.18×10^{-8}
Linear	1218	1	4.87×10^{-16}	1.08×10^{-7}

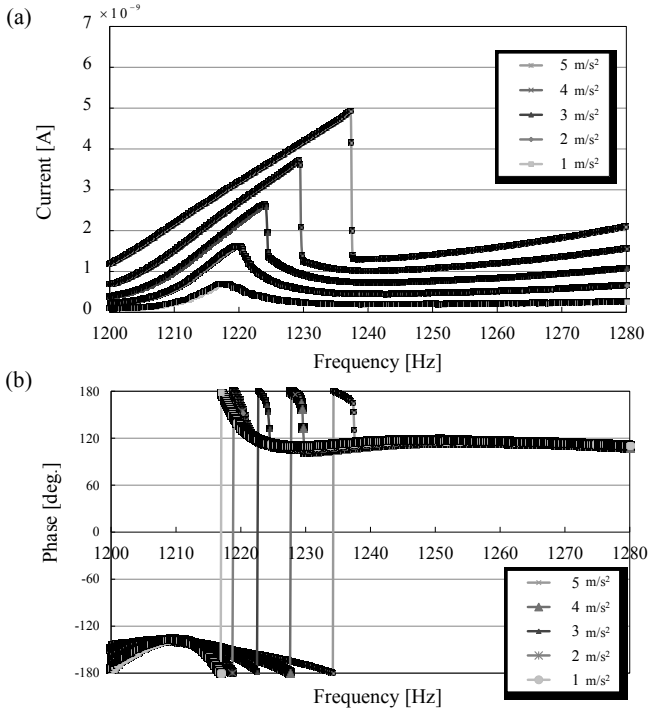

Fig. 7. Current generation results for frequency response: (a) current dependence of the acceleration for external vibration and (b) phase dependence of the acceleration.

VI. SUMMARY

A MEMS electrostatic energy harvester was fabricated by using thick-multilevel interconnection technology. For the movable structure of the vibrational device, the nonlinear oscillation was demonstrated by the energy harvester with a conventional electret made of ETFE film. It generated a 4.93 nA current for nonlinear wideband oscillation at a resonance frequency of 1238Hz. To reveal the nonlinear effect, we introduced a derivation for the energy harvester effectiveness, The value is 9.6 times larger than that for the linear operation.

ACKNOWLEDGMENT

The authors thank Mr. Alexander Hwang Yu of Georgia Institute of Technology, Dr. Hiroki Morimura of NTT Device Innovation Center, Prof. Hiromu Ishii of Toyohashi Institute of Technology, and Prof. Katsuyuki Machida of Tokyo Institute of Technology for useful discussions and encouragement throughout this study. They also thank Mr. Keisuke Yoshioka for measuring the mechanical characteristics and electrical properties of the fabricated devices.

REFERENCES

[1] Iker Mayordomo, Peter Spies, Fritz Meier, Stephan Otto, Sebastian Lempert, Josef Bernhard and Alexander Pflaum, "Emerging technologies and challenges for the Internet of Things," IEEE 54th int. Midwest symp. On circuits and systems (MWSCAS), pp.1-4, Aug., 2011.

[2] Ryota Negishi, Kentaroh Toyoda, and Iwao Sasse, "Opportunistic routing protocol with grid-based relay slot selection in energy harvesting WSNs," Proc. of APCC, pp. 412-416, Oct., 2014.

[3] A. Harb: "Energy harvesting: State-of-the-art," Renew. Energ. vol. 36, p p. 2641-2654, 2011.

[4] N. Sato, K. Ono, T. Shimamura, K. Kuwabara, M. Ugajin, S. Mutoh, H. Morimura, H. Ishii, J. Kodate, and Y. Sato: "Energy harvesting by MEMS vibrational devices with electrets," Proc. 15th Int. Conf. Solid-State Sensors, Actuators and Microsystems (IEEE Transducers), p p. 513-516, June, 2009.

[5] K. Ono, N. Sato, T. Shimamura, M. Ugajin, T. Sakata, S. Mutoh, and Y. Sato: "A millimeter-sized electret-energy-harvester with microfabricated horizontal arrays and vertical protrusions for power generation enhancement," Proc. 16th Int. Conf. Solid-State Sensors, Actuators and Microsystems (IEEE Transducers), pp. 1863-1866, June, 2011.

[6] K. Ono, N. Sato, T. Shimamura, M. Ugajin, T. Sakata, S. Mutoh, J. Kodate, Y. Jin, and Y. Sato: "Synchronized multiple-array vibrational device for microelectromechanical system electrostatic energy harvester," Jpn. J. Appl. Phys. Vol. 51, pp. 05EE01-1-6, 2012.

[7] N. Sato, K. Ono, T. Shimamura, K. Kuwabara, M. Ugajin, and Y. Sato: "Analysis of electret-based MEMS vibrational energy harvester with slit-and-slider structure," J. Microelectromech. Syst. vol.21, pp.1218-1228, 2012.

[8] T. Shimamura, M. Ugajin, K. Suzuki, K. Ono, N. Sato, K. Kuwabara, H. Morimura, and S. Mutoh: "Nano-watt power management and vibration sensing on a dust-size batteryless sensor node for ambient intelligence applications," Dig. Tech. Pap. IEEE Int. Solid-Stage Circuits Conf., pp. 504-505, Feb., 2010.

[9] T. Shimamura, M. Ugajin, K. Kuwabara, K. Takagahara, K. Suzuki, H. Morimura, M. Harada, and S. Mutoh, "MEMS-switch-based power management with zero-power voltage monitoring for energy accumulation architecture on dust-size wireless sensor nodes," Proc. of VLSI Circuits, pp.276-277., 2011.

[10] H. Morimura, T. Shimamura, K. Kuwabara, K. Ono, and K. Machida, "Integrated CMOS-MEMS technology and its applications", IEICE, Vol. J95-C, No.8, pp. 175-182, 2012.

[11] F. Braghin, F. Resta, E. Leo, and G. Spinola, "Nonlinear dynamics of vibrating MEMS," Sens. Actuators A, vol. 134, pp. 98-108, 2007.

[12] F. Cottone, H. Vocca, and L. Gammaitoni, "Nonlinear energy harvesting," Phys. Rev. Lett., vol. 102, pp.080601-4, 2009.

[13] D. Miki, M. Honzumi, Y. Suzuki, and N. Kasagi, "Large-amplitude MEMS electret generator with nonlinear spring," IEEE 23rd Int. Conf. MEMS, pp. 176-179, Jan., 2010.

[14] R. L. Harne and K. W. Wang, "A review of the recent research on vibrations energy harvesting via bistable systems," Smart Mater. Struct., vol. 22, p. 1, 2013.

[15] I. Kozinsky, H.W.Ch. Postma, O. Kogan, A. Husain, and M.L. Roukes, "Basins of attraction of a nonlinear nanomechanical resonator," Phys. Rev. Lett., vol. 99, p.207201, 2007.

[16] S.C. Stanton, C.C. MacGehee, and B.P. Mann, "Nonlinear dynamics for broadband energy harvesting: Investigation of a bistable piezoelectric inertial generator," Phys. D, vol. 239, pp. 640-643, 2010.

[17] P. Basset, D. Galayko, A. Mahmood Paracha, F. Marty, A. Dudka, and T. Bourouina: "A batch-fabricated and electret-free silicon electrostatic vibration energy harvester," J. Micromech. Microeng., vol.19, pp. 115025-12, 2009.